

Surface properties of inorganic materials

LOW-FIELD ELECTRON EMISSION AND CATHODE LUMINESCENCE OF PIEZOELECTRIC FILMS OF OXIDES AND CHALCOGENIDES

A.A. Dadykin¹, A.G. Naumovets¹, P.P. Gorbik², I.V. Dubrovin²,
V.M. Ogenko², and M.N. Filonenko²

¹*Physics Institute, National Academy of Sciences
Prospekt Nauki 46, 03028 Kyiv-28, UKRAINE*

²*Institute of Surface Chemistry, National Academy of Sciences
Gen. Naumov Str. 17, 03680 Kyiv-164, UKRAINE*

Abstract

Basic parameters of effective low-field emitters of electrons of piezoelectric films for bright flat cathode luminescent display and other activity are optimised. Specimens of electron emitters of cathode luminescent screens are based on compounds of SiO₂, ZnO, ZnS, solid solution of Zn_{1-x}Cd_xS. High efficient "cold" emitters of electrons were prepared on the basis of mono- and polycrystalline films. The emission and cathode-luminescent properties of the films were investigated. It is shown that developed films are perspective like the flat displays with the brightness of 300 Cd/m².

Introduction

According to the classical theory of autoemission of metals and semiconductors, electric fields near a surface of emitters to produce measurable currents are needed with $E > 10^7$ V/cm. However, in a series of runs it was registered appearance of the electron emission for $E > 10^5$ V/cm estimated from macrogeometry of electrodes (so-called LFEE - low-field electron emission). It was established experimentally that the appearance of LFEE can be explained neither a simple geometric strengthening of an electric field over microprojections of surface nor a local diminution of work function, nor a suggested, in the case of diamond, presence of areas on the emitting surface, having the natural negative electron affinity (NEA).

The direct experiments have established [1] that a main, insertion less in fact, component of LFEE is due to the presence on the emitting surface of filmy dielectric formations with a great ratio of longitudinal sizes to thickness. Visual observations and a secondary ion mass-spectrometry have shown that the formations consisted of commination products of cathode luminophores fabricated from the compounds of A^{II}B^{VI} type, from anode screen of the experimental diode cell, or from oxides of SiO₂ type remaining on the chemical etching out of cathodes. Both silicon dioxide and cathode luminophores, as it is known, are good piezoelectrics. In this connection it was proposed, that had found an experimental support, that as a result of deformations under an electric field there appear contact electric fields on faces of piezoelements exceeding 10^7 V/cm. For such external fields in the near-surface region of emitters, in case of a low dielectric constant (in piezoelectrics $\epsilon \sim 5$), internal fields reach values of $10^6 - 10^7$ V/cm too, for which the Zener_effect is possible, and

electrons can exit to vacuum immediately out of the valence zone of a piezoelectric. Evidently, in order to realise this situation it is necessary an enough perfection of specimens - a general requirement for technology of piezoelectric.

It is interesting to trace a relationship of LFEE with piezoeffect on the example of specimens of the $A^{II}B^{VI}$ -type compounds and silicon dioxide which are relatively readily can be prepared in a form of glasses, ceramics, textures and monocrystals with a sharply differing piezoelectric activity. Along with it, owing to the temperature and temporal stability of physical parameters, a development of technologies of field emitters on their basis presents a practical interest. Preliminary runs have shown that current density at the quartz cathode exceeds 10 A/cm^2 (the best barium oxide cathodes give $\sim 1 \text{ A/cm}^2$), and such cathodes can be used in fabrication of bright flat cathode-luminescent panels-displays.

Procedure of measurements and experimental specimens

Experimental devices are made as autoelectronic Muller projectors to study emission from separate areas of points and diode cells with flat cathodes and anode-screens coated with cathode luminophores of the $A^{II}B^{VI}$ -type for visualisation of emission. Cathode-anode distances were ordinarily of ~ 100 microns, and operating voltages - of several kV, so that average electric fields in a cell reached 10^6 V/cm . Upon such field mechanical stresses appear in piezoactive films that exceed considerably the electrostriation ones resulting in degradation of the cathode luminophore and pollution of the cathode. In this connection, there were designed and prepared, by the method of evaporation in a quasi-closed volume, filmy cathode luminophores of ZnO and films of solid solution of $Zn_{1-x}Cd_xS$ with a good adhesion enduring without a marked degradation electron flows over 1 W/cm^2 . Efficiency of cathode luminescence at a voltage of 400 V was about 3 Lu/W that is comparable to the efficiency of low-voltage powdered luminophores of the ZnO:Zn type. The objects of studies were:

1. Oxide films on the surface of silicon points that were prepared by treating blanks in nitric acid.
2. Submicronic layers of SiO_2 formed in electroadsorption of oxygen on silicon at $\sim 10^6 \text{ V/cm}$.
3. "Mushroom-shaped" SiO_2/SiO structures that were formed while fabricating multipoint silicon cathodes.
4. Multielement matrix structures of a textured SiO_2 that were produced by a final oxidation applied through masks onto metallised glass plates.
5. Monocrystalline quartz plates (piezoresonance quartz pick - up of the industry production).
6. Quartz and sapphire glasses.
7. Polycrystalline filmy textured structures of zinc oxide produced by the method of oxidation of zinc selenide and sulfide.
8. Textured films of zinc sulfide.
9. Textured films of solid solution of $Zn_{1-x}Cd_xS$.

Field electron emission from the piezoactive SiO_2

Fig. 1 gives an autoemission image of the silicon point with an atomically clean apex and hardly stable to vaporisation oxide film at its foot. Autoemission characteristics in coordinates $\lg i = f(1/V)$ (FN-characteristics) of different areas of the point differ sharply both qualitatively and quantity. The current of films at the points foot ($E \sim 10^5 \text{ V/cm}$) is many orders higher than that of the face (111) on the apex ($E > 10^7 \text{ V/cm}$), and a FN-characteristic of emission has a well-defined fracture reflecting differences in mechanisms of emission from several of the emitter.

Transformation of FN characteristics as the silicon point with the atomically clean surface oxidises by the way of electroadsorption of oxygen at $E \sim 10^6$ V/cm are presented in Fig. 2. The fracture appears when the continuous oxide film of $\sim 500\text{\AA}$ thickness is formed.

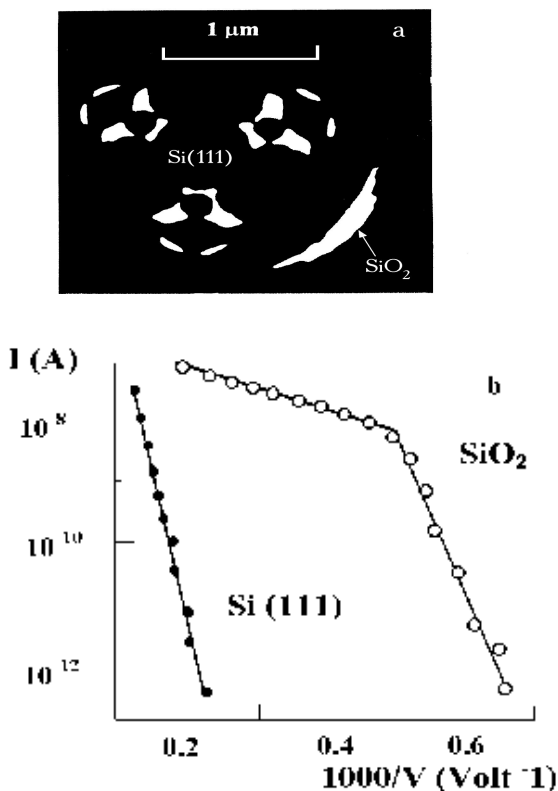


Fig. 1. Autoemission characteristics of the field emission from the atomically clean face (111) of silicon (*a*) and from the oxide formation at the points foot (*b*).

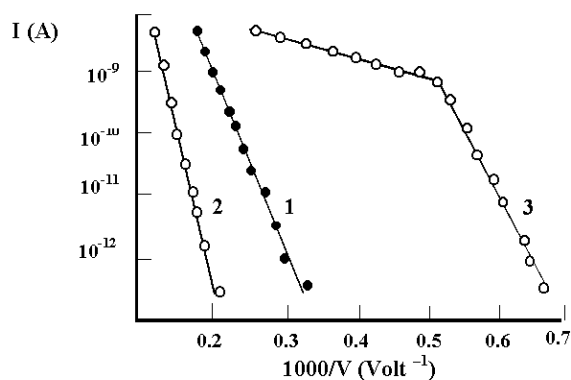


Fig. 2. Transformation of characteristics of field emission of the Si-cathode as oxygen is electroadsorbed: 1- the atomically clean surface, 2- a monolayer of oxygen, 3 - for the thickness of a SiO₂ film $\sim 500\text{\AA}$.

Of special interest are emission properties of "mushroom-shaped" system of SiO₂ given in Fig. 3. Emission is observed from edges of oxide "hats", but completely corroded points with the hats removed do not emit.

Geometry of emitting elements is distinguished by a great proportion of longitudinal sizes to thickness and can be easily reproduced in a filmy variant. Film elements in a form of

matrices of the textured SiO_2 having a varied shape and dimension are prepared by the final oxidation of SiO in air at $T=700\text{K}$. Emission was observed from edges of elements with the greatest sizes in the matrix with elements of different sizes.

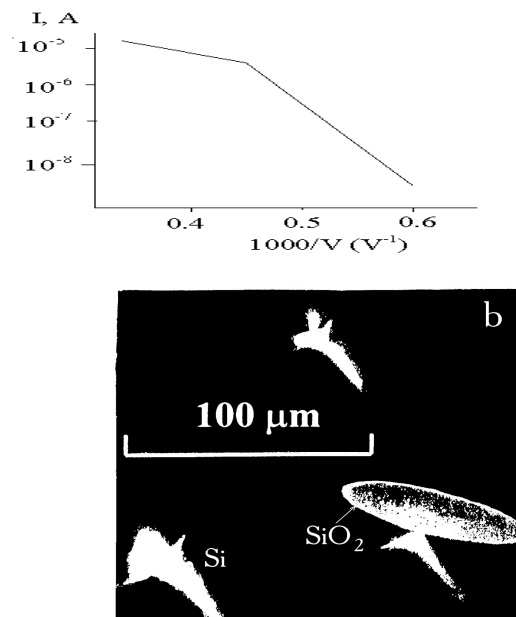


Fig. 3. Characteristics of field emission from the end of the oxide film on a silicon leg of the "mushroom-shaped" emitter.

Because it has been established that for LFEE were essential not absolute sizes of elements, but their ratios, so elements of centimetre sizes were tested. For this purpose, monocrystalline quartz piezoresonance pickups were used (Fig. 4) with metallic electrodes for supply of a polarising voltage. Emission was not detected up to values of electric field near the surface of piezoelement exceeding 10^6 V/cm in the absence of the polarising voltage. With the supply of a polarising voltage as early as for the polarisation field of $<10^5 \text{ V/cm}$ there was recorded a stationary electron emission from the end of piezoelement in direction of one of electric axes of quartz. The emission image of the piezoelement in the anode - screen coated with ZnS cathode luminophore is shown in Fig. 4.

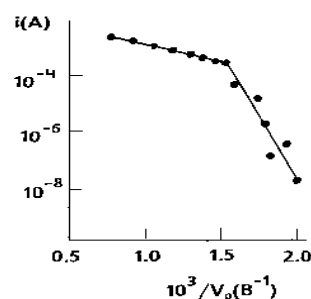


Fig. 4. A characteristic of field emission from the end of quartz piezoresonator at voltage in the anode - screen 2kV. V_p - a polarising voltage in plates of resonator.

With a change in polarity of the voltage in electrodes, emission is observed in the direction of another electric axis turned about 120° . When the value of a polarising voltage is changed, the image turns smoothly in the plane of piezoelement that indicates to the existence of shear piezopolarisation. FN-characteristic as in all above-mentioned cases has a fracture, and a current density estimated from the geometry of specimen, exceeds 10 A/cm.

In the case of specimens fabricated from evidently non-piezoelectric fused silica and sapphire, emission is not detected even for polarising field of $>10^6$ V/cm. Attention is attracted to a high stability of LFEE in the field of great emission currents even for $p \sim 10^{-5}$ Torr, that is important for practical applications. Fig. 5, a gives a simple explanation of the results obtained.

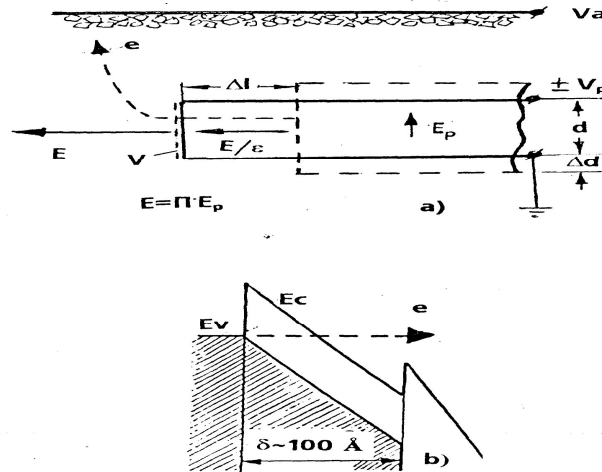


Fig. 5. (a) - On a mechanism of piezogeometrical amplification of the electric field near the end of piezoelement, Π - a factor of piezogeometrical amplification; (b) - An energetic scheme of the piezofield emission in the field of large emission currents.

The piezoelement in a form of plate with sizes l and thickness d in a polarising field E_p deforms so that end faces and side surfaces find themselves under different potentials, proportional to absolute deformations. Here

$$V/V_p = \Delta l / \Delta d = \sigma l / d \quad (1)$$

where σ is the Poisson coefficient.

The contact field arising at the end may be estimated as

$$E \sim (V - V_p)/d = 4\pi k^2 \sigma l/d E_p = \Pi E_p \quad (2)$$

where k - a coefficient of the electromechanical bond. Under experimental conditions $\sigma \sim 0.5$; $k \sim 0.5$; $l/d \sim 10^3$, so that $\Pi > 100$. It means that the E field can exceed 10^7 V/cm for the polarising field $E_p \sim 10^5$ V/cm. In this case an internal field E/ϵ for low ϵ can attain values of 10^7 V/cm sufficient to develop the internal electric breakdown (Zener effect), and the condition of the effect NEA is realised on the emitter surface with the field-penetrating inside. The energetically scheme of the field emitter in such a situation is shown in Fig. 5, b. This model of emitter explains both a course of FN characteristics and a high stability of emission for high currents: for low voltages the emission is limited by a potential barrier on the boundary to vacuum and considerable fluctuations of current appear due to adsorption of residual gases, but for high ones - the source of electrons (a valence band) becomes hidden of the external medium by the protective film of piezoelectric.

Emission and cathodoluminescent properties of zinc oxide films prepared by the method of oxidation of zinc selenide and sulfide

Zinc oxide possesses a number of physical and chemical properties and finds a wide application in the world-wide production of adhesives, paints, glasses, piezoelements etc [2]. Of the particular interest is its use in the electrotechnical and electron industry as piezoelectric in the form of ceramics, films and crystals [3-5]. Manufacture of the materials indicated is connected with certain difficulties, since zinc oxide possesses a high melting temperature and a low pressure of saturating vapours. Of considerable interest is the use of polycrystalline films of zinc oxide as components of photodetectors of UV radiation [6] and luminescent materials [7,8]. To produce films, high-temperature technologies are used such as evaporation and condensation of the starting material [9] by an electron beam [10], by the method of magnetron sputtering [11]. The use of these methods complicates a control of physical properties, disturbs stoichiometry of the material. Particular difficulties appear in the synthesis of films and coats in the case of using profiled supports as well as supports with a low temperature of melting. We studied physicochemical conditions of formation of polycrystalline layers of zinc oxide from zinc-containing precursor - zinc sulfide and selenide by means of oxidation. Also were studied the possibilities of using the prepared films as emitters and anode - screens of cathodoluminescent displays. The essence of the chosen technological method consists in the use of light-volatile zinc compounds as the precursor. These properties belong to its chalcogenides, which, along with a well-developed technology of their production (in particular, sulfide, selenide and solid solution on their basis), possess an insignificant (<1 mol %) mutual solubility with zinc oxide at temperatures of over 1000°C [12].

The starting films of zinc sulfide and selenide were prepared by evaporation and condensation under vacuum of 10^{-5} mm Hg. Temperatures of stable to vaporisation and support varied in the ranges of 800-850°C and 100-150°C, respectively.

Oxidation of films of zinc chalcogenides was performed in a flow system with oxygen at temperature of 300-450°C. The oxygen underwent the preliminary drying and purification. Temperatures of processes of synthesis and oxidation were controlled with accuracy to ± 0.1 K by means of a precision programmable regulator of RIF-101 type.

The chemical composition and morphology of films was studied by a scanning electron microscope with a X-ray spectral microanalyzer of ICXA-733 type and Auger-spectrometer IAMP-IOS (JEOL firm).

Study of the structure and the phase composition of films were carried out by means of diffractometer DRON-3M with CuK_α -radiation.

Flat and profiled plates of glass were used as supports, including the glass coated with a transparent electroconducting layer of tin oxide.

Optimum regimes were selected in order to sputter films of zinc chalcogenides of 0.3-10 μ thick using the above-mentioned method, which possessed a minimum number of microdefects. It was established that the composition of films (in limits of the measuring error) was close to the composition of starting compounds.

During the oxidation reaction of chalcogenide films, the transformation of a sphalerite lattice of chalcogenides into a wurtzite one - a typical of zinc oxide and having changes in parameters of a crystal unit cell. This, as well, possibly, the lack of agreement between coefficients of thermal expansion of a support and film resulted in the formation of a polycrystalline coating of zinc oxide. At this point a quality of films, i.e., the presence of macrodefects and transverse pores increases. In this connection, oxidative process of chalcogenide films for different temperatures was studied in detail. Optimum results have been obtained for the isothermal oxidation of zinc selenide at temperature of 400°C.

Fig. 6 gives dynamics of the oxidative process of the zinc selenide film. The absence of coinciding, the most intense, reflexes of zinc selenide and oxide made it possible to observe well the kinetics of a topochemical oxidation reaction:

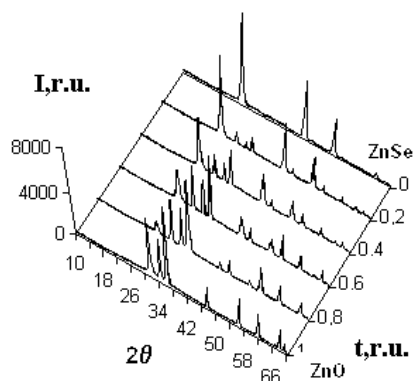


Fig. 6. Dynamics of oxidation of zinc selenide by data of X-ray phase analysis.

During the course of experiment it was established that a dependence of a transformation degree in the oxidation reaction of ZnSe on time at $t=400^{\circ}\text{C}$ has typical sigmoid form.

The transformation degree was determined by a calibration curve obtained for processing the data on measurement of intensity of reflexes for a mechanical mixture of the ZnO-ZnSe system. Kinetic regularities were analysed using equations by B.V. Erofeev [13] for the growth of spherical nuclei which number increases at a constant rate in a form

$$\alpha = 1 - \exp(-Kt^n) \quad (4)$$

where α - is a degree of transformation, K - is a constant, t - time, $n = \sigma + a$, σ - has a meaning of the number of elementary stages when a nucleus transforms in the actively growing nucleus, and depends on the number of directions in which nuclei grow. An n - constant entering the equation was found by treatment of experimental data using the relationship

$$\ln[-\ln(1 - \alpha)] = \ln K + n \ln t \quad (5)$$

Since $\ln[-\ln(1 - \alpha)]$ depends linearly on $\ln t$, then by a tangent of angle of slope of this straight line it can be determined the parameter n , which value allows to judge about mechanism of oxidation of zinc chalcogenides.

The value of $n=4.2$ close to 4 is the evidence that the growth of nuclei develops in three directions for the one stage change of a nucleating centre into the actively growing nucleus. The deviation of experimental dependence from linear in the initial stage of the transformation process points to a complex nature of oxidative mechanism for this stage. In order to improve adhesion of ZnO films etchers for supports have been selected. The best results for the thermoadding have been obtained in case of films of zinc oxide synthesised on a glass support pretreated by boiling in bichromate, and then by treatment for 5 min in 5% hydrofluoric acid at the standard temperature as well as glass specimens coated with tin oxide by boiling for 5 min in 10% alkaline solution followed by careful washing in the distilled water and drying.

The use of films of zinc sulfide and selenide as precursors makes possible to produce while oxidation them with oxygen in a flow system, quality textured films of zinc oxide, devoid of macrodefects and with a controlled stoichiometry.

As is known, textured ZnO films under certain technological conditions of their production have high values of piezomodules and coefficients of the electromechanical

coupling. According to [1] highly efficient piezofield emitters operating steadily even for $p \cong 10^{-5}$ Torr can be produced on the basis of these films. On the other hand, zinc oxide is an efficient cathode luminophor. So, studies of emission and luminescent properties of ZnO have been performed in devices, in which a cathode and anode are made of the same material, with regard to requirements to its stoichiometry. Such a performance of the checking diode allows avoiding a vacuum possible contaminations during measurements. The measurements have been carried out in a flat diode cell of 1×1 cm size and with gap of $\cong 100 \mu$ to ensure average field strengths of $> 10^5$ V/cm. The results of measurements are presented in Fig. 7 with the Fauler-Nordheim dependence (FN characteristic).

It attracts attention a high stability of emission in the range of large emission currents even for $p = 10^{-5}$ Torr. It is due to the fact that large ($\cong 10^7$ V/cm) electric fields are created in complete films of piezoelectric's in a near-surface field of $\cong 100 \text{ \AA}$, great enough to develop the Zener effect, for which a source of electrons becomes a valence band of piezoelectric (the electron source is hidden from an outer medium with a protective film of the piezoelectric).

A potential barrier on a boundary limits the emission with vacuum in the range of low currents. Here, the emission is not stable because of great fluctuations of work function caused by adsorption of residual gases. A current density from separate elements of the matrix exceeded 10 A/cm^2 ; a full current to anode - screen reached 1 mA for $E_{cp} \cong 10^5$ V/cm. The emission differed also by a high spatial uniformity for a high stability in the region of high currents ($> 90\%$ elements emitted simultaneously).

The ZnO-Zn film of cathode luminophor for a high adhesion endured without visible breakdown electron flows more that 1 W/cm^2 . The efficiency of film cathode luminescence is comparable with efficiency of a powdery cathode luminophor ($\approx 3 \text{ Lu/W}$). For such parameters of a powdery cathode and anode it is readily attained a brightness of the cathodoluminescent screen, $\approx 300 \text{ Cd/m}^2$ that is two orders more than the brightness of the electroluminescent screen.

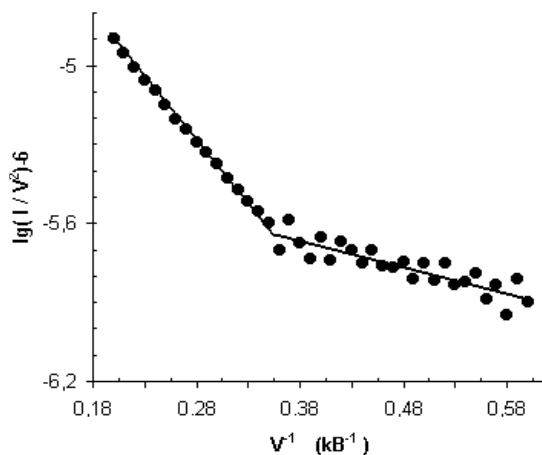


Fig. 7. A FN-characteristic of 100-element film ZnO emitter prepared by oxidation of zinc selenide.

Changes in emission and luminescent properties of ZnO films were not found during pretreatment of operating mock-ups of displays for hundreds of hours.

It should be noted that in the case of ZnO films as well AlN films, which were amorphous by data of X-ray phase analysis, no electron emission was found even for middle electric fields exceeding 10^6 V/cm.

The similar situation appears as well in the case of films of cubic modification for normal to a support orientation of axis of the fourth-order symmetry which is nonpiezoactive

that confirms too the fact of emergence of the low-field electron emission as a result of the piezoelectric amplification of electric field.

Thus, the described technology can be used in development of highly efficient piezofield cathodes for devices of vacuum micro- and nanoelectronics of different purposes.

Flat cathodoluminescent displays based on ZnS:CdS thin films

Films of a solid solution $Zn_{1-x}Cd_xS$ of a different composition ($0 < x < 1$) were prepared on dielectric supports (glass, glass with a thin layer of SnO_2 or a metal) using a thermal evaporation in a quasi-closed volume from autonomous sources: polycrystalline tablets of zinc and cadmium sulfide. As starting components, powders of ZnS and CdS were used that the chemical industry releases. Chambers of a vacuum apparatus maintained a pressure of $1.33 \cdot 10^{-2} - 6.65 \cdot 10^{-3}$ Pa in the working volume. A choice of geometric sizes of the reactor was determined by sizes of the working chamber of the vacuum aggregate and a temperature field of oven. The chemical composition of the resulting films was determined by results of the X-ray phase analysis, by a spectral distribution of photoconduction as well as by a spectral distribution of photosensitivity of specially fabricated heterostructures. Temperatures of evaporators and supports during evaporation were controlled by means of platinum-platinum/rhodium and chromel-alumel thermocouples. The temperature of supports was changed within 150-300°C. The temperature of sources was changed within 700-950°C for cadmium sulfide and within 800-1080°C for zinc sulfide. Horizontal screens with incompatible openings were situated in the reactor between the support and evaporator.

The crystalline structure of the resulting films was found to depend on their composition. The films of zinc sulfide had a cubic structure despite the fact that in the initial state the wurtzite phase was predominant in the ZnS structure. The value of parameter for the cubic unit cell a ZnS films that is equal to 5.412 Å was consistent well to the cited references ($a = 5.406$ Å). The films of solid solutions of $Zn_{1-x}Cd_xS$ on the part of ZnS had a sphalerite structure and, if make a note of intensity of reflexes, 1-2% wurtzite phase. For higher concentrations of cadmium sulfide a structure of $Zn_{1-x}Cd_xS$ films were a wurtzite one. All the films examined were oriented partially what can be judged by the ratio of reflexes and their quantity. It should be noted that diffractograms of films obtained under the same technological regimes are identical that is the evidence of a sufficient reproduction of the elaborated procedure of $Zn_{1-x}Cd_xS$ film production.

The composition of the films studied was determined by values of lattice parameters of solid solutions using the graphical dependence for polycrystalline samples as well as by the spectral dependence of photosensitivity of heterojunction of $pCu_2 - nZn_{1-x}Cd_xS$ (with this in view there have been made heterojunctions which photosensitivity was due to the intrinsic absorption of emission in $Zn_{1-x}Cd_xS$). It is known that the width of a forbidden gap of solid solutions of $Zn_{1-x}Cd_xS$ varies depending on the composition by the linear law. The composition of films was determined, basing on this the position of a "red" boundary of photoeffect in heterojunction. The results obtained are fairly consistent with the data of X-ray phase analysis on the investigation of photoconductivity of $Zn_{1-x}Cd_xS$ films. Lattice parameters of solid solution of $Zn_{1-x}Cd_xS$ films being studied and their chemical composition are given in Table 1.

The study of microstructure of produced films by means of the metallography microscope revealed the existence of the explicitly expressed polycrystalline structure, the character of which depended on preparative conditions and composition of solid solution. Thus, $Zn_{1-x}Cd_xS$ films of a differing composition but approximately of equal thickness ($\sim 10\mu$) deposited on the same supports at the same temperatures, had a differing microstructure. The structure of films was granular one, the grain size was decreased as a concentration of zinc sulfide in a solid solution was increased. The grains had a crystalline facet. One has found that

the grain size depended apparently on the support temperature and increased with the temperature rise. The study in the polarised light hag showed that these films were textured partly. Texturization of the films prepared might be due to the predominant growth of favourably oriented nuclei.

Table 1. The structure of $Zn_{1-x}Cd_xS$ as function of composition.

Films number	Composition (in mol %)		Type of crystal structure	Lattice parameters, Å, a+0.006
	ZnS	CdS		
1	—	100	wurtzite	4.142
2	14	86	wurtzite	4.092
3	24	76	wurtzite	4.066
4	27	73	wurtzite	4.060
5	47	53	wurtzite	3.990
6	57	43	wurtzite	3.962
7	78	22	sphalerite	5.508
8	100	—	sphalerite	5.412

It was established for a transverse chip that crystallites had in height a columnar form, their thickness increased with the growth of a film thickness. Surface of the transverse microsection of films do not have microcracks, void inclusions or micropores. Grain boundaries have a dense cohesion and a sufficiently high mechanic strength that allows the film together with a conducting sublayer to be deformed without any failure. Optimal for making matrix luminescent displays turned out to be the films of $Zn_{1-x}Cd_xS$, which have a polycrystalline structure with a middle size of crystallites, 2-6 μ . At this point, the height of columnar crystallites was commensurate with the film thickness.

The $Zn_{1-x}Cd_xS$ films have electron conductance (that was checked by the method of thermoprobe and by the Hall effect) because, perhaps, that in the process of growth there occurs self-activation of the solid solution by excessive cadmium. The specific resistance of films is $\sim 10^4$ to 10^{10} Ohm·cm, increasing for an increased concentration of ZnS in the solid solution.

Measurements of the Hall effect were carried out for $Zn_{1-x}Cd_xS$ films that contain in the solid solution up to 20 mol % zinc sulfide (when concentrations of zinc sulfide in the solid solution are large, the resistivity of the films was increased abruptly that prevented from making measurements).

The experimental results demonstrate that the n concentration of free carriers (of electrons) in films depends substantially on the temperature of warming - up a support. On rising the support temperature, n diminishes. The highest-resistant films of $Zn_{1-x}Cd_xS$ are produced at temperatures of the support of $\sim 180-220^\circ\text{C}$. The optimum temperatures are about $200 - 220^\circ\text{C}$ for which are observed a favourable combination of polycrystalline structure and electrophysical parameters of films $Zn_{1-x}Cd_xS$ solid solution. In the investigated area of composition of base films, the concentration of free electrons depends weakly on the concentration of zinc sulfide in a solid solution and amounts for different samples $10^{11}-5 \cdot 10^{16} \text{ cm}^{-3}$. The value of mobility ranges from 10 to 15 cm/Vs. Low values of carriers mobility can be explained by the high density of grain boundaries and other defects of the crystal structure of the $Zn_{1-x}Cd_xS$ films (dislocation, intrinsic and exemplary defects).

The experimental dependence of the width of forbidden gap of $Zn_{1-x}Cd_xS$ on the composition is given in Table 2. The synthesised solid solutions have a great practical interest for needs of vacuum micro- and nanoelectronics: on the one hand, these, as

piezoelectronics, can be used for fabricating highly efficient cold sources of electrons for different purposes, and on the other hand, as efficient cathode luminophors for full-colour screens of television sets of a high sharpness.

Table 2. The dependence of the width of forbidden gap of $Zn_{1-x}Cd_xS$ on the composition.

Composition (in mole %)		E_g , eV
ZnS	CdS	
0	100	2.25
20	80	2.50
40	60	2.75
60	40	3.00
80	20	3.25
100	0	3.50

The visualization and measurements of the electron emission have been carried out in a flat diode cell having a size $1 \times 1 \text{ cm}^2$ and an inter electrode gap of $\sim 100 \mu\text{m}$. The average electric fields in the gap could be brought up to $\sim 10^6 \text{ V/cm}$. The thin film cathode and anode (screen) were prepared from solid solutions $Zn_{1-x}Cd_xS$ obtained by thermal evaporation from autonomous ZnS and CdS sources heated in a quasi-closed chamber. The thickness of the films was 0.3 to 3 μm . In another version of the technique, the films were deposited by evaporation of a mixture of ZnS and CdS powders filling a platinum crucible

Choosing the content of the components as well as the temperatures of the evaporators and substrates could control the ratio between the wurtzite (piezoactive) and sphalerite phase in the films. The phase composition was determined by X-ray phase analysis and by spectral measurements of the photoconductivity. The microstructure of the films was investigated by optical and scanning electron microscopy.

Depending on the deposition conditions, the resistivity of the films could be varied within the range 0.01 to 10^{10} Ohm cm . The resistivity as well as the adhesion of the films depended also on the properties of the conducting metal sublayer. We tested Ta, Cr, Mo, and Ni. Suitable properties were found for the sublayers prepared by evaporation of a Cu-Ag alloy.

To fabricate the matrices of “single-unit” emitting elements ($0.3 \times 0.3 \text{ mm}^2$), the glass plates previously coated with a metal sublayer and $Zn_{1-x}Cd_xS$ thin film, were locally abraded in such a way as to create the corresponding “pattern”.

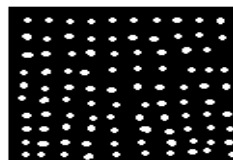


Fig. 8. Field emission pattern of a 100 element matrix cathode ($1 \times 1 \text{ cm}^2$).

The matrices with the elements of the “pixel” type (100 emitters per pixel) were prepared by evaporation through metal masks. The noise and response characteristics of the electron emission were measured using a high-sensitive fluctuation technique developed in our laboratory.

Fig. 8 shows a typical emission image of a 100-element matrix cathode visualised on a $Zn_{1-x}Cd_xS$ thin film cathodoluminescent screen. Varying the film composition could vary the

colour of the image from blue to red. The film sustained, without any appreciable destruction, the electron fluxes up to 1 W/cm^2 , which allowed us to obtain the brightness of the luminescence above 300 Cd/m^2 comparable to the brightness of powder phosphors. Such a high brightness may be caused by the mosaic structure of the film.

The cathode film whose emission is depicted in Fig. 11 contained about 90% of the wurtzite modification and its resistivity amounted to 10^9 Ohm cm . The electrically active axis had a predominant orientation normal to the surface. The separate elements of the matrix shaped as squares $0.3 \times 0.3 \text{ mm}^2$ in size were deposited onto conducting Cu stripes, which gave the possibility to scan the image line by line. Fig. 8 shows the emission distribution when all the elements are switched on simultaneously. It is estimated that above 90% of the elementary emitters give comparable currents. To attain such a high degree of the spatial uniformity of emission in the case of metal tip arrays, it is necessary to provide each tip with an individual current-limiting resistor. This requirement results in additional complication of technology.

Fig. 9 depicts a typical current-voltage dependence of the total emission current from a cathode matrix plotted in the Fauler-Nordheim (FN) coordinates. The dependence was recorded under the pressure of residual gases of $\sim 10^{-5} \text{ Torr}$, and exhibited a remarkable emission stability in the region of high emission currents. To attain such a high stability within the whole range of the currents, a vacuum of $\sim 10^{-10} \text{ Torr}$ is necessary. The total current from the matrix amounted to 1 mA and was limited by cracking of the glass substrate of the screen. It is estimated that the current density from an individual emitting element of the matrix is $\geq 10 \text{ A/cm}^2$ at the field (measured macroscopically) $E \leq 10^5 \text{ V/cm}$. The operating parameters of the model display described above demonstrate the possibility of fabrication of both single-element and many-element (pixel) displays of this type. The specific choice depends on the requirements for image brightness, dimensions and information capacity of the display. To fabricate a matrix of single-element emitters, a technology should be used which ensures a narrower spread in the size of the elements (e.g. photolithography).

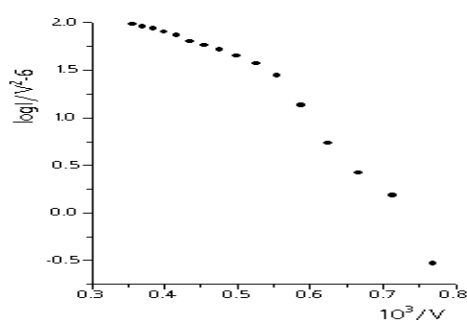


Fig. 9. F-N plot of a matrix field emitter at $P=10^{-5} \text{ Torr}$. Integrated current from matrix is 1 mA at $E_{av}=3 \cdot 10^5 \text{ V/cm}$. Current density from one emitting spot is $j > 10 \text{ A/cm}^2$.

The emission characteristics of the piezoactive thin film cathodes can be interpreted in terms of a potential diagram shown in Fig. 10. At low voltages, the emission is limited by the transparency of the potential barrier at the boundary thin of film-vacuum. The strong current fluctuations observed in this case are caused by adsorption of residual gases. At high voltages, when the electric field penetrates the film, the condition of the effective negative electron affinity is realized at the surface.

At high fields, due to penetration of the field into emitter and band bending, the EA becomes negative ($\chi_{ef} > 0$, the diagram on the left) and the current becomes stable (see the upper segment of the FN plot). The electric field within the film due to its piezogeometrical

enhancement can attain a value of $\sim 10^7$ V/cm, which is sufficient for the Zener effect in the dielectric. Such a situation can arise near the edges of a thin film with a piezoelectric activity where a considerable amplification of the electric field should come into effect. This possibility was exemplified in [1] for SiO₂, ZnS, ZnO and CdS piezoelectric films. Due to field-induced inclination of the energy bands the operating source of electrons is protected by the film and the surrounding gas atmosphere does not practically affect the emitter operation.

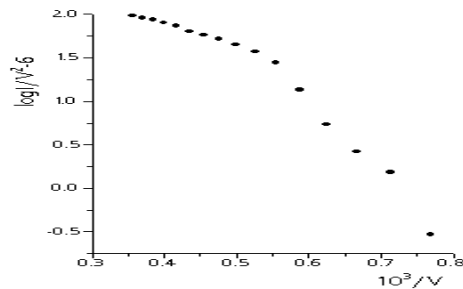


Fig. 10. At low fields, the electron affinity (EA) of the emitter is positive ($\chi_{ef} > 0$, see the diagram on the right), and the emission current shows powerful fluctuations (see the strong scatter of the points in the FN plot at low currents).

The spatial uniformity of the emission is probably provided by the circumstance that the emitting films itself, which can be readily prepared, rather uniform over the entire emitter surface, serves a current limiting resistor.

Conclusions

This study, after carrying out many investigations, basing on examples of specimens of a different configuration and chemical composition, has established that a stationary low inertial ($\varepsilon < 10^{-7}$ s) macroscopically low-field ($E_{cp} \sim 10^5$ V/cm) electron emission appeared only in the case of samples being made of piezoelectric materials of a high degree of stoichiometry and purity. In the case of non-piezoelectric materials (glass, fused silica, sapphire, amorphous films of A^{II}B^{VI}), or the films of A^{II}B^{VI} produced, from data of X ray diffraction analysis, in a sphalerite modification at a normal to support orientation a non-piezoelectric axis of the fourth order, no emission was registered for even middle fields exceeding 10^6 V/cm. In the case of non-piezoelectric diamond-like films with a high content of donor defects, although emission is registering for $E_{middle} \sim 10^5$ V/cm, however it differs by a big ($\sim 10^{-3}$ s) time lag and a high level of flicker – noise [14]. From the results above-mentioned it is seen that for emergence of the insertion less emission not absolute sizes of samples are essential, rather a ratio of their longitudinal sizes to a thickness. Strong electric fields ($> 10^7$ V/cm) appear for a high (~ 100) ratio of these sizes near edges of the samples fabricated from piezoelectric materials, and in the near surface region for a low ($\varepsilon \sim 10$) dielectric constant, electron fields are enough to develop Zener effect. The energetic scheme of emission corresponding to this case explains insensitivity of emission to vacuum condition: a source of electrons - a valence band - is hidden from an external medium.

In addition, methods for preparation of films used in this study - after oxidation of sulfides as well as the method of evaporation in a quasi-closed volume - give the possibility to produce highly effective film cathode luminophors with a controllable chromacity.

The 100-element matrix display that has been made through these methods, for a high homogeneity of emission had a brightness of cathode luminescence exceeding 300 Cd/m². High (~ 10 A/cm²) local densities of currents from cathodes of piezoelectric materials give the

possibility for making on their basis also other articles of vacuum microelectronics such as powerful miniature reception - amplifying and generator valves, cathodes of electron microscopes, etc. Thus, the results of this study make it possible to deepen understanding of the mechanism of a mysterious phenomenon of quick response low field emission and can be used for development of various articles of electrovacuum technique based on prospective piezoelectric.

Acknowledgement

This work has been supported by the Ministry of Ukraine for Education and Science (Project N5.1.04453).

References

1. Dadykin A.A. On mechanisms of a low-field electron emission // *Pis'ma v Zhur. Experm. Teor. Fiz.* – 1997. - V.65, N11. - P.823-827.
2. Perl Allen S. Zinc oxide // *Amer. Ceram. Soc. Bull.* - 1996. – V.75, N6. - P.162-165.
3. Novrega M.C. Varistor performance of ZnO-based ceramics related to their densification and structural development // *J. Amer. Ceram. Soc.* - 1996. – V.79, N6. - P.1504-1508.
4. Wei-I Lee Applications of deep level transient spectroscopy and depth profile measurements on polycrystalline zinc oxide ceramic // *Abstr. Mater. Res. Soc. Fall Meet. Boston. Mass., Nov. 27-Dec. 1, 1995.* -Boston (Mass), 1995. - P.T8.11.
5. Izaki M. and Omi T. Transparent zinc oxide films chemically prepared from aqueous solution // *J. Electrochem. Soc.* - 1997. - V.144, N1. - P.L3-L5.
6. Rensmo H., Kais K., and Lindstrom H. High light-to energy conversion efficiencies for solar cells based on nanostructured ZnO electrodes // *J. Phys. Chem. B.* -1997. - V.101, N14. - P.2598-2601.
7. Kynev K., Maneva N., and Gridorov L. Luminescence of ZnO:Sm doped with cation impurities // *Dokl. Bulg. AN.* - 1996. – V.49, N2. - P.37-40.
8. Vanheusden K. Correlation between photoluminescence and oxygen vacancies in ZnO phosphors // *Appl. Phys. Lett.* - 1996. - V.68, N3. - P.403-405.
9. Rouanet A. and Solmon H. Synthesis by vaporization-condensation and characterization of γ -Fe₂O₃, In₂O₃, SnO₂, ZnO, Zr_{1-x}Y_xO_{2- δ} // *Nanostruct. Mater.* - 1995. – V.6, N1-4. - P.283-286.
10. Walg Q. Structural properties of non-stoichiometric zinc oxide films deposited by E-beam evaporation technique // *Journal of Nanjing. Univers. Natur. Sci. Ed.* -1996. – V.32, N3. - P.410-413.
11. Abduev A.H., Magomedov A.V., and Shakhmaev Sh.O. Formation of zinc oxide layers using a magnetron sputtering // *Izv. AN. SSSR Neorgan. Mater.* -1997. – V.33, N3. - P.340-343.
12. Tomashik V.N. and Grishchiv V.I. State Diagrams of Systems Based on Semiconductor Compounds of A^{II}B^{VI}. -Kiev: Naukova Dumka, 1982 (in Russian).
13. Boldyrev V.V. Effect of Crystal Defects on Rate of Thermal Decomposition of Solids. Tomsk: Ed.TSU. - 1963. - P.114-145 (in Russian).
14. Dadykin A.A. and Naumovets A.G. A study of time and space correlations in field emission current fluctuation with a fiber-optical technique. *Acta Phys. Polonica A.* – 1992. - V.81, N1. - P.131-143.